Surface chemical control of the electronic structure of silicon nanowires: Density functional calculations

Paul W. Leu,* Bin Shan, and Kyeongjae Cho†
Stanford University, Stanford, California 94305, USA
(Received 6 February 2006; revised manuscript received 1 April 2006; published 23 May 2006)

Silicon nanowires (NWs) have potential use in many electronic and photonic applications. In this study, we have systematically investigated the modification of Si NW electronic structure for different sized NWs and different surface coverage (H, Br, Cl, and I) using *ab initio* density functional theory calculations. The surface chemistry is shown to have strong effects, comparable to that of quantum confinement, on the band structure of Si NWs. Electronic structure analysis reveals the primary cause of the band gap change is the suppression of surface states as determined by the strength of the surface bonds. The results elucidate surface chemical control of NW electronic structure and illustrate an example of simulation-based design characterization of nanoelectronic components.

DOI: 10.1103/PhysRevB.73.195320 PACS number(s): 78.67.Lt, 73.22.−f

Recent developments in vapor liquid solid growth methods[1] have made possible the synthesis of semiconductor nanowires (NWs) with precise control. Semiconductor NWs have emerged as a potential building material for a diverse variety of electronic and optical applications, such as light emitting diodes,[2] lasers,[3] and optical interconnects. These small-sized NWs not only provide for increased sensitivity, higher density devices, and better functionality, but also have the potential for integration with existing Si microelectronics.

Si NWs have quite different electronic structure from their bulk crystalline counterpart due to quantum confinement. While bulk Si is a poor optoelectronic material due to its indirect band gap, Si NWs can have a direct band gap and optical activity has been observed experimentally.[4–6] The quantum confinement effect gives rise to visible photoluminescence[7] and its enlargement of band gap in H-terminated NWs has been experimentally observed.[8] A number of theoretical calculations[9–12] have also been performed to study the quantum confinement effect in Si NWs, mostly on ⟨100⟩ oriented NWs with rectangular cross sections terminated with H. These studies have shown that quantum confinement becomes significant for NWs with diameters less than 3 nm.

While the effect of quantum confinement on Si NW band structure has been explored extensively, the use of Si NW surface modification for band structure engineering has received less attention despite its potential importance. Si surface modification is frequently used in microelectronic device processes. In porous Si, the existence of different surface species such as polysilanes or SiH_x,[13] siloxene molecules,[14] and nonbridging oxygen hole centers[15] has been proposed to be responsible for photoluminescence. Some computational studies have shown the importance of oxygen[16,17] and other passivants[18] in Si nanoparticles. Similarly, the large surface-to-volume ratio in Si NWs can be exploited in NW functionalization and used to modify transport properties in applications such as sensors[19,20] and addressing arrays.[21] Si NWs tend to form a layer of SiO_2 with thickness 1–2 nm under ambient conditions,[1] and subsequent HF treatment can be used to remove this oxide layer and terminate the surface with Si-H bonds. A number of different Si surface treatments can be performed and it is also energetically favorable to passivate Si surfaces with halogens (Cl, Br, and I).[22] However, the effects of surface chemical modification of Si NW electronic structure have not been systematically investigated.

In this study, we report a first-principles study on the effects of different surface species (H, Cl, Br, I) on the band gap of Si NWs. The NWs we studied range from 0.6 to 3 nm in diameter and have different growth directions. It was found that the band gaps of Si NWs with different types of surface passivation can differ by up to a few eV, comparable to those due to quantum confinement. Such variation is more pronounced for NWs that are smaller and those with surface coverage above 50%. The reduction in band gap is shown to be correlated with the existence of surface states due to the surface bonding species. Based on the calculations, we present the idea of using surface coverage as a degree of freedom in modifying the band structure of Si NWs.

We considered NWs with four different growth directions: the ⟨111⟩, ⟨110⟩, and ⟨112⟩ are growth directions that have been observed experimentally,[8] as well as the ⟨100⟩ growth direction, which most previous first-principles studies have focused on.[11,23–25] The NWs were cut using the low free-energy (111), (100), and (110) facets consistent with Wulff construction[26] and experimental observations.[27] The NW cross sections are illustrated in Fig. 1(b). The calculations were done using density functional theory (DFT) within the generalized gradient approximation (GGA)[28] and projector augmented wave pseudopotentials[29] using the Vienna Ab Initio Simulation Package (VASP). The NWs are put in a supercell with a cross section of 45×45 Å^2. At this unit cell size, the interwire distance is >8 Å, which effectively prevents the overlapping of wave functions from neighboring cells. The Kohn-Sham single-electron wave functions are expanded by plane waves with a cutoff energy of 245.3 eV. We used four Monkhorst-Pack k points along the axis of the NW. The whole geometry was relaxed within the supercell until the forces on each atom are less than 0.1 eV/Å.

Figure 1(a) illustrates the band gaps for different sized H-terminated NWs in various growth directions, where the

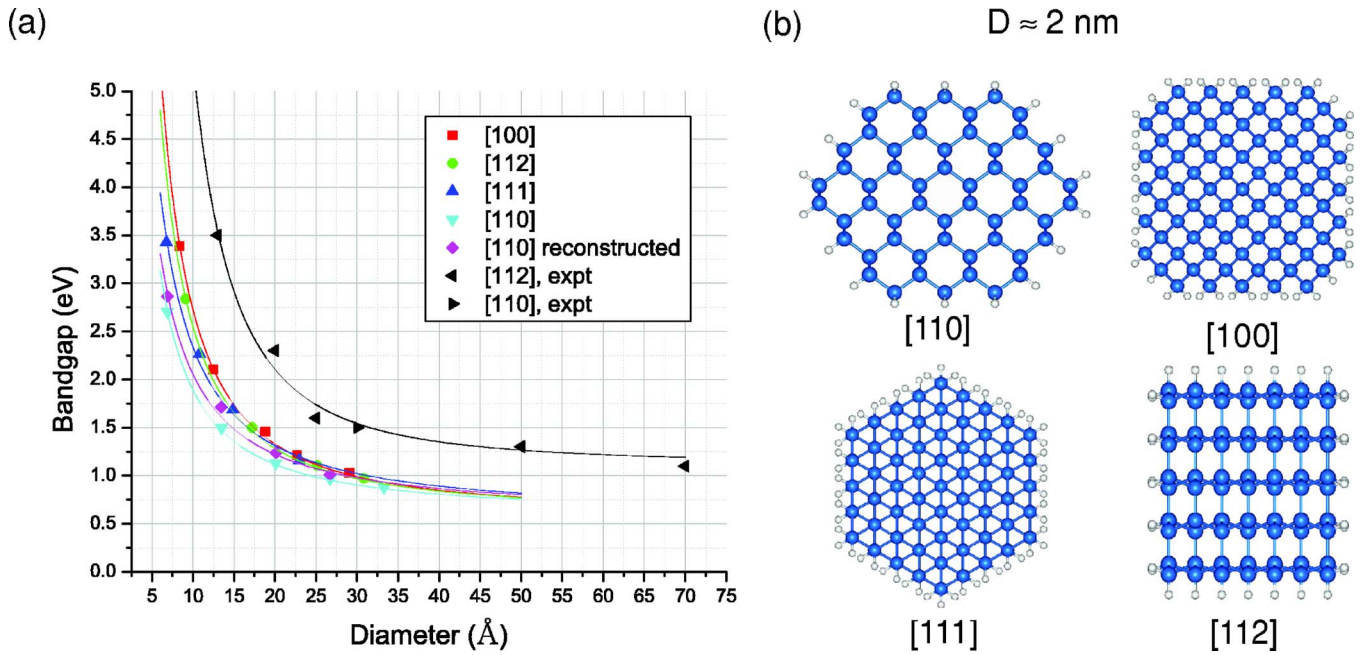

FIG. 1. (Color online) Band gaps of H passivated NWs in different growth directions. (a) displays the band gaps as a function of diameter, while (b) shows the cross section of the NWs.

cross sections of these different growth directions are displayed in Fig. 1(b). The band gap E_g for the NWs is such that $E_g^{\langle 110\rangle} < E_g^{\langle 110\rangle \mathrm{re}} < E_g^{\langle 111\rangle} < E_g^{\langle 112\rangle} < E_g^{\langle 100\rangle}$. In addition, we note that the $\langle 110\rangle$ and $\langle 100\rangle$ NWs are direct band gap, while the $\langle 111\rangle$ and $\langle 112\rangle$ NWs are indirect, consistent with the band-folding approximation. The data points have been fitted to $E_g^{hkl} = A/d^n + E_g^{\mathrm{bulk}}$, where E_g^{bulk} is the GGA bulk band gap of Si=0.6 eV and A and n are fitting parameters. While DFT within the local density approximation is known to underestimate band gap, more accurate quantum Monte Carlo calculations have shown that DFT reproduces the general trends of band gap change.[30] We obtained values of n in the range of 1.2–1.6 from our fitting, close to $n=2$ corresponding to the effective mass approximation.

The correlation between surface structure and electronic properties can be seen in the (100) surface reconstruction of $\langle 110\rangle$ NWs (denoted $\langle 110\rangle$re). The (100) facets were reconstructed by removing a pair of H atoms from neighboring Si atoms and forming an additional Si-Si bond, as shown in Fig. 2(b). We observed that $2\times 1(100)$ surface reconstruction in

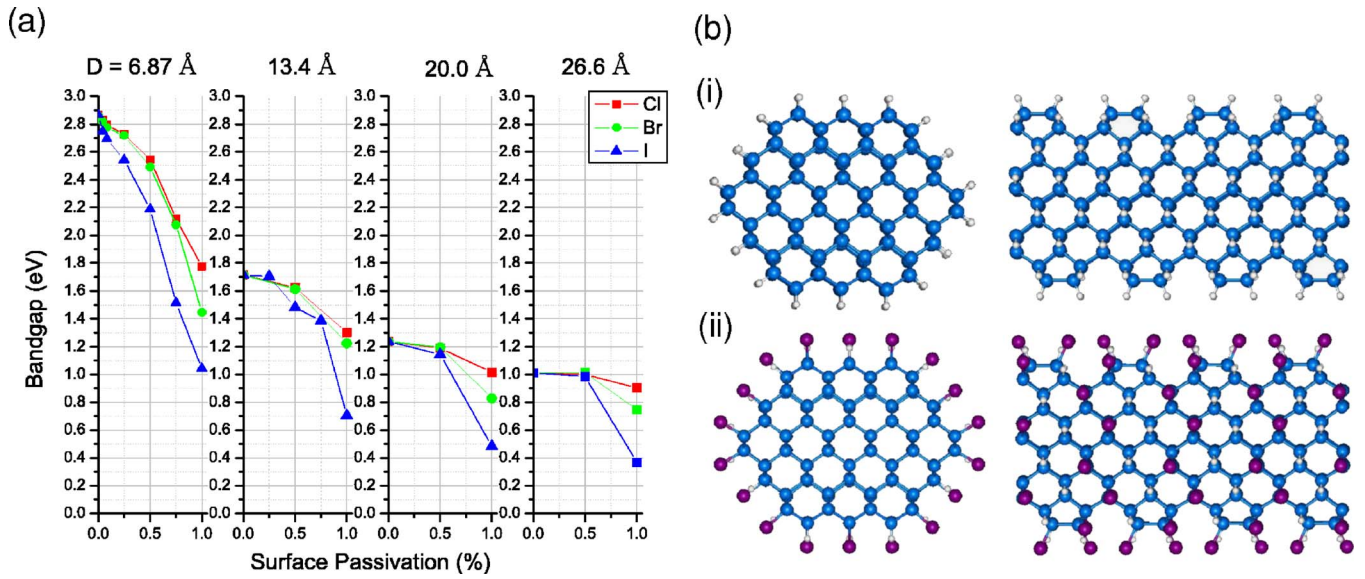

FIG. 2. (Color online) Band gaps of H passivated NWs at different diameters as a function of surface coverage %. Surface passivation has the strongest effect at smaller diameters and at passivation above 50% coverage. (a) displays the band gaps as a function of surface coverage at different diameters, while (b) displays the structure of the 2 nm diameter NWs at 100% H coverage and 50% I coverage.

TABLE I. Reaction energy for 6.9 Å diameter NW at different surface coverage. The reaction energy for each surface coverage is calculated with the reactants of the Si NW with H passivation and I_2, while the product is the Si NW with appropriate passivation and H_2. Other halogen species and different size NWs exhibit similar trends.

Surface coverage (%)	Reaction energy (eV/at)
4	−0.77
8	−0.76
25	−0.68
50	−0.64
75	−0.61
100	−0.54

NWs leads to a band gap enlargement of a few tenths of an eV. In contrast, small Si nanoparticles have been reported to exhibit a redshift in band gap after (100) surface reconstruction.[17,31] Surface reconstruction leads to localized surface states that behave like impurity levels. Puzder *et al.* note that these surface states reside within the band gap for small nanoparticles, leading to an optical gap of 3.5 eV with weak size dependence. However, NWs are confined in one less dimension than nanoparticles and our smallest ⟨110⟩ NWs have a band gap of 2.7 eV. The states from the surface dimers reside outside the band gap of these NWs. In fact, NW (100) surface reconstruction leads to a slightly larger band gap because the effective size of the NW is slightly reduced and, hence, confinement is slightly stronger. After reconstruction, the NW conduction- and valence-band edge

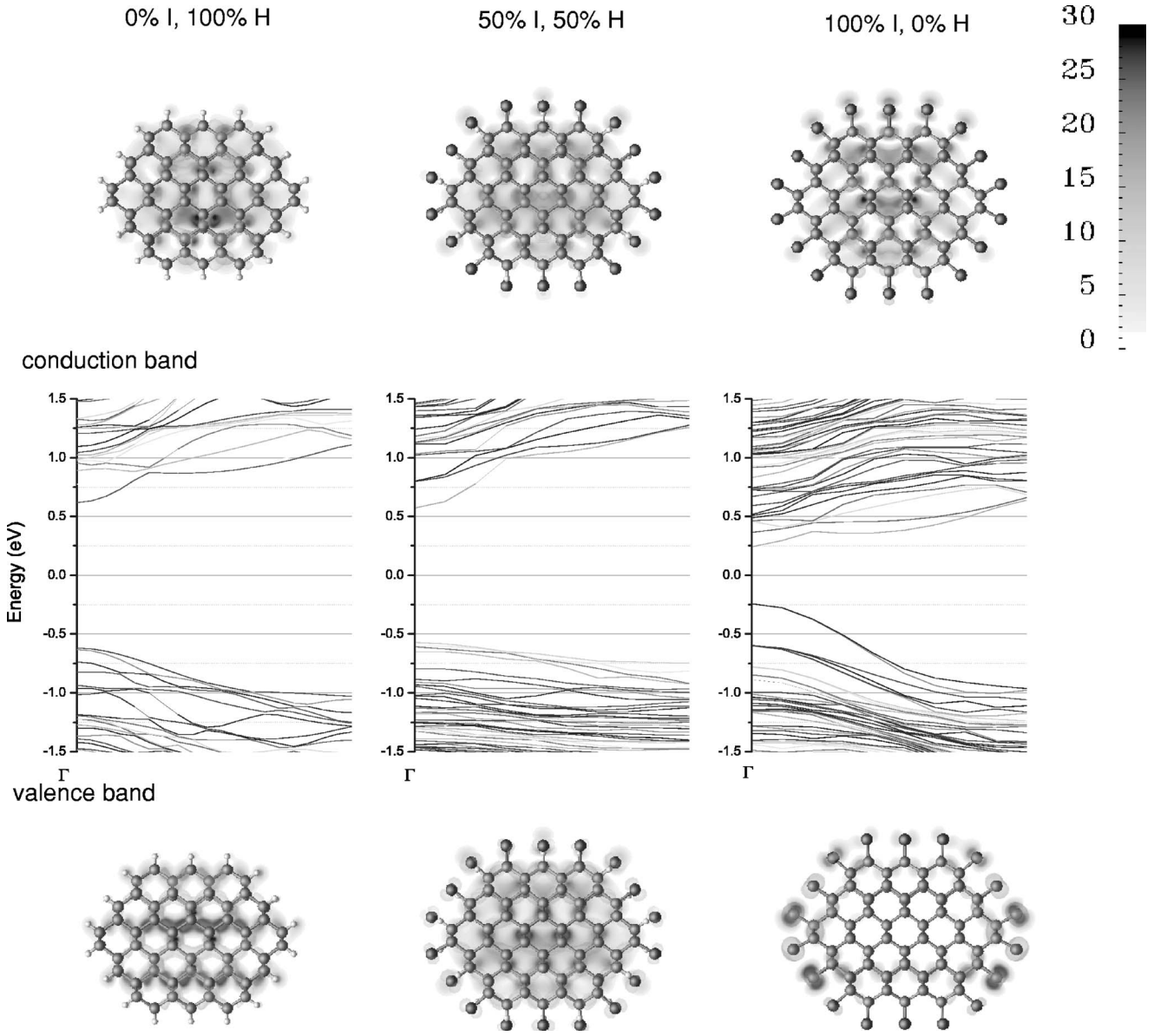

FIG. 3. Band structure of I passivated NWs about 2 nm in diameter at 0%, 50%, and 100% I coverage. The band structures and conduction-band minimum and valence-band maximum states show similar trends for different diameters and different surface passivation species at the same coverage %. The charge density multiplied by the volume $[\rho(r) \times V_{\text{cell}}]$ with units of Coulombs of the valence-band and conduction-band states is shown below and above the band structure plots. $V_{\text{cell}} \approx 7760$ Å^3. $\rho(r) = 0.09$ C/Å^3 is shown in light gray.

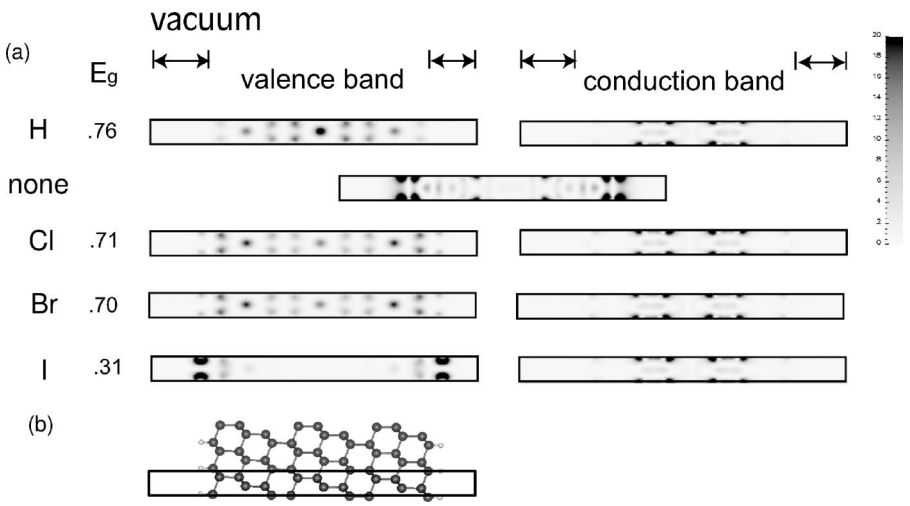

FIG. 4. Partial charge density of the valence-band maximum and conduction-band minimum for an Si slab of about 3 nm thickness with H, no passivation, Cl, Br, and I passivation. The partial charge density is in units of Coulombs after being normalized by the volume of the unit cell $\rho(r) \times V_{\text{cell}}$. $V_{\text{cell}} \approx 544$ Å^3. The valence- and conduction-band states have bulklike character to them when the slabs are passivated with H. With weaker bonding, the valence-band and conduction-band states become more surfacelike. (b) shows the structure of one of the slabs.

states cannot hybridize with the surface states from the reconstructed Si dimer and do not extend to the reconstructed (100) surfaces.

To study the effects of different surface passivations in more detail, we focused on ⟨110⟩re NWs since ⟨110⟩ is the most common growth direction for NWs from 3 to 10 nm in diameter[27] and it is energetically favorable to reconstruct the (100) surfaces. It should be mentioned that the results we present in the following are general and apply well to NWs with other growth directions. We have investigated the passivation of NWs with halogen atoms (Cl, Br, I), which are all stable methods of passivating Si surfaces. Fluorene is kinetically unstable on Si and Ge surfaces due to its high polarity and thus is not included in the calculation. Table I lists the heat of reaction for I atoms on Si NW surfaces. We note that the reaction is exothermic and that it should be possible to obtain 100% coverage on these NWs. With increasing surface coverage, the binding affinity is weaker, but the driving force continues to be toward 100% surface coverage as the stability of the H_2 molecule in the reaction products helps drive the NWs to halogenate. Other halogen species show similar trends and are more exothermic.

Figure 2 depicts the band gap modification of NWs using these halogens for different diameters at different surface coverage (0%, 50%, and 100% for all NWs and some more surface coverages for smaller NWs). The geometry of 50% passivated NWs is shown in Fig. 2(b), where the halogen atoms alternate with H atoms along the NW axis. Under the same percentage of passivation, I has the strongest reduction of the band gap, followed by Br and then Cl. The bonding strength of Si NWs and these halogen atoms are in exactly the opposite order of band gap reduction. The bond lengths of the different passivation species are about 1.51 Å for H, 2.07 Å for Cl, 2.24 Å for Br, and 2.46 Å for I. Cl has the greatest reaction energy followed by Br, and then I. We also note that the halogens on the (100) reconstructed surface are about 3.86 Å apart from each other.

The observed band gap modification by surface passivation can be understood from band structure analysis. Figure 3 depicts the details of the band structure modification of a 2 nm diameter Si NW with different amounts of I passivation. We note that for H passivated Si NWs, the valence-band maximum and conduction-band minimum states are concentrated more in the interior of the wire. Similar effects have been observed in studying H passivated NWs versus free surface NWs.[32] With increasing halogen passivation, the conduction-band minimum and valence-band maximum states are spread out more toward the surface of the NW. With 100% halogen passivation, the conduction-band minimum state is now located in both the internal part of the NW and the (100) surfaces, and the valence-band maximum is now concentrated on the (110) surfaces. NWs of different diameter with the same surface coverage show similar trends.

To see more concretely the existence of surface states and the origin of band gap reduction, we perform calculations on Si slabs of about 3 nm thickness with H, no passivation, Cl, Br, and I passivation. The charge density of the valence-band maximum (VBM) and conduction-band minimum (CBM) are displayed in Fig. 4. With H passivation, the VBM and CBM are concentrated more in the interior of the slab, having bulklike character. Without passivation, the surface states are located in the midgap of the slab. H exhibits strong bonding with Si and pulls the surface states out of the band gap into the conduction and valence bands. With the different surface halogen passivations, Cl, Br, and I, weaker bonding strength between the surface species and Si results in a smaller band gap and increasingly more surfacelike character to the VBM and CBM. The change in VBM is more significant than that from the CBM.

It is also observed that band gap reduction is more rapid at high surface coverage. Above 50% surface passivation, the halogens become nearest neighbor along the axis direction and start interacting more strongly with one another. This

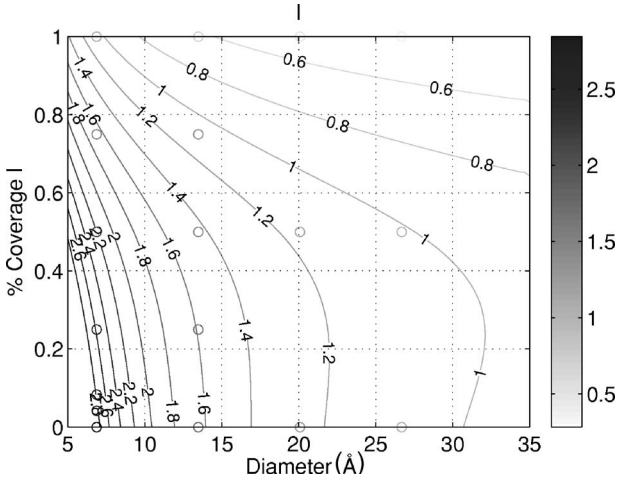

FIG. 5. Contour plot of the band gaps of I passivated NWs.

interaction weakens the bonding of the halogen atom with the Si NW, resulting in a reduced band gap. Figure 5 depicts a contour plot of the band gap of NWs as a function of diameter and surface I passivation. The circles indicate actual data points to which the contours are interpolated using biharmonic spline interpolation.[33] The contours are produced by curve fits of $E_g^{hkl}=A/d^n+C$ for 0%, 50%, and 100% surface coverage and contours are produced using interpolation. The shape of the contours indicates that the band gap change is most significant at >50% surface coverage and diameter changes are most significant under 30 Å. This plot is an example of simulation-based design and can be used to guide band gap engineering.

In conclusion, we have studied the effects of different surface passivation on the band structure of Si NWs. It was found that the coverage of more weakly interacting surface species leads to a larger band gap reduction. The origin of band gap reduction comes from the surface species weakly interacting with the NW and thus not pulling the surface states as far out of midgap. The passivation of halogens is energetically favorable and allows for a new method for engineering the electronic states of Si NWs.

The authors would like to thank the San Diego Supercomputer Center for computational resources and the Stanford Nanowire Facility for helpful discussions. P.L. would like to thank Stanford University and the NSF for financial support. The authors would also like to thank the NSF Center of Integrated Nanomechanical Systems (COINS) for financial support.

*Electronic address: pleu@stanford.edu
†Electronic address: kjcho@stanford.edu

[1] A. M. Morales and C. M. Lieber, Science **279**, 208 (1998).
[2] Y. Huang, X. F. Duan, and C. M. Lieber, Small **1**, 142 (2005).
[3] X. F. Duan, Y. Huang, R. Agarwal, and C. M. Lieber, Nature (London) **421**, 241 (2003).
[4] Y. W. Wang, C. H. Liang, G. W. Meng, X. S. Peng, and L. D. Zhang, J. Mater. Chem. **12**, 651 (2002).
[5] J. Huo, R. Solanki, J. L. Freeouf, and J. R. Carruthers, Nanotechnology **15**, 1848 (2004).
[6] H. Pan, W. Z. Chen, S. H. Lim, C. K. Poh, X. B. Wu, Y. P. Feng, W. Ji, and J. Y. Lin, J. Nanosci. Nanotechnol. **5**, 733 (2005).
[7] A. Cullis, L. Canham, and P. Calcott, J. Appl. Phys. **82**, 909 (1997).
[8] D. D. D. Ma, C. S. Lee, F. C. K. Au, S. Y. Tong, and S. T. Lee, Science **299**, 1874 (2003).
[9] S. Horiguchi, Physica B **227**, 336 (1996).
[10] H. Yorikawa, H. Uchida, and S. Muramatsu, J. Appl. Phys. **79**, 3619 (1996).
[11] B. Delley and E. F. Steigmeier, Appl. Phys. Lett. **67**, 2370 (1995).
[12] X. Zhao, C. M. Wei, L. Yang, and M. Y. Chou, Phys. Rev. Lett. **92**, 236805 (2004); F. Bruneval, S. Botti, and L. Reining, *ibid.* **94**, 219701 (2005); X. Zhao, C. M. Wei, L. Yang, and M. Y. Chou, *ibid.* **94**, 219702 (2005).
[13] S. M. Prokes, O. J. Glembocki, V. M. Bermudez, R. Kaplan, L. E. Friedersdorf, and P. C. Searson, Phys. Rev. B **45**, 13788 (1992).
[14] M. S. Brandt, H. D. Fuchs, M. Stutzmann, J. Weber, and M. Cardona, Solid State Commun. **81**, 307 (1992).
[15] S. M. Prokes and W. E. Carlos, J. Appl. Phys. **78**, 2671 (1995).
[16] M. V. Wolkin, J. Jorne, P. M. Fauchet, G. Allan, and C. Delerue, Phys. Rev. Lett. **82**, 197 (1999).
[17] I. Vasiliev and R. M. Martin, Phys. Status Solidi B **233**, 5 (2002).
[18] A. Puzder, A. J. Williamson, J. C. Grossman, and G. Galli, Phys. Rev. Lett. **88**, 097401 (2002).
[19] Y. Cui, Q. Q. Wei, H. K. Park, and C. M. Lieber, Science **293**, 1289 (2001).
[20] X. T. Zhou, J. Q. Hu, C. P. Li, D. D. D. Ma, C. S. Lee, and S. T. Lee, Chem. Phys. Lett. **369**, 220 (2003).
[21] Z. H. Zhong, D. L. Wang, Y. Cui, M. W. Bockrath, and C. M. Lieber, Science **302**, 1377 (2003).
[22] J. M. Buriak, Chem. Rev. (Washington, D.C.) **102**, 1271 (2002).
[23] F. Buda, J. Kohanoff, and M. Parrinello, Phys. Rev. Lett. **69**, 1272 (1992).
[24] A. J. Read, R. J. Needs, K. J. Nash, L. T. Canham, P. D. J. Calcott, and A. Qteish, Phys. Rev. Lett. **69**, 1232 (1992).
[25] T. Ohno, K. Shiraishi, and T. Ogawa, Phys. Rev. Lett. **69**, 2400 (1992).
[26] S. Hong and M. Y. Chou, Phys. Rev. B **57**, 6262 (1998).
[27] Y. Wu, Y. Cui, L. Huynh, C. J. Barrelet, D. C. Bell, and C. M. Lieber, Nano Lett. **4**, 433 (2004).
[28] M. C. Payne, M. P. Teter, D. C. Allan, T. A. Arias, and J. D. Joannopoulos, Rev. Mod. Phys. **64**, 1045 (1992).
[29] G. Kresse and D. Joubert, Phys. Rev. B **59**, 1758 (1999).
[30] A. J. Williamson, J. C. Grossman, R. Q. Hood, A. Puzder, and G. Galli, Phys. Rev. Lett. **89**, 196803 (2002).
[31] A. Puzder, A. J. Williamson, F. A. Reboredo, and G. Galli, Phys. Rev. Lett. **91**, 157405 (2003).
[32] C. Y. Yeh, S. B. Zhang, and A. Zunger, Phys. Rev. B **50**, 14405 (1994).
[33] D. T. Sandwell, Geophys. Res. Lett. **14**, 139 (1987).